LIP-STUDENTS-24-6

Production and characterization of cell-level passive dosimeters

Gabriel Lente[1] and Miguel Quiaios[2]

[1] *Nova School of Science and Technology|FCT NOVA, Lisboa, Portugal*
[2] *Instituto Superior Técnico (IST), Lisboa, Portugal*
[3] *Laboratório de Instrumentação e Física Experimental de Partículas (LIP). Lisboa, Portugal*
[4] *Faculdade de Ciências. Universidade de Lisboa (FCUL), Portugal*
[5] *Centro de Ciências e Tecnologias Nucleares (C2TN). Departamento de Engenharia e Ciências Nucleares (DECN). Instituto Superior Técnico (IST). Universidade de Lisboa. Lisboa. Portugal*

Project supervisor: Cristiana Rodrigues[3,4,5], João Gentil Saraiva[3], António Pereira Gonçalves[5] *November 5, 2024*

Abstract. Al_2O_3 crystals can be used as passive dosimeters with micrometer resolution in radiation therapy, personal and facility dosimetry, and radiobiology research. Al_2O_3 crystals were produced using the flux method and characterized with UV-Vis photospectroscopy and scanning electron microscopy (SEM). The effect of crystal growth temperature was investigated, with growth at 1140 ºC achieving the best results. The OSL response to the radiation was studied for crystals with different combinations of dopants and flux purity. The results demonstrated that higher-purity flux and some dopants, like carbon and titanium, significantly enhanced OSL response, and there are different OSL responses for doses below and above 25 Gy.

Keywords: Dosimetry, Alumina Crystals, Flux Method, OSL Dosimetry

1 Introduction

The Al_2O_3 crystals register radiation with induced changes in the crystal's structure, which can be verified with an absorption spectrum and quantified using optically stimulated luminescence (OSL). They can also work as fluorescent nuclear track detectors (FNTD), which have demonstrated a promising performance for dosimetry of neutrons (if a converser is used), protons and other heavy charged particles. [1]

In the present study, the crystals were produced using the flux method, which was chosen over the more common Czochralski method because of its simplicity. The variables tested were the temperature at which the crystals are grown and the purity of the flux.

In this work 3 groups of crystals were used: commercial Al_2O_3:C,Mg crystals, which were thoroughly described and studied previously [2–4]; Al_2O_3 crystals with diverse dopant combinations; and the undoped Al_2O_3 crystals produced for this study.

Diverse dopant combinations were evaluated, since Al_2O_3:C and Al_2O_3:C,Mg have presented better OSL dosimetry capabilities than Al_2O_3 [2]. The dopant combinations explored were: C; C,Mg; C,Mn; C,Zn; C,Ti. Furthermore, the effect of the flux purity in the OSL properties was studied with two batches (Al_2O_3 and Al_2O_3:C,Mg) being produced with a 99.5% purity flux, instead of the 99% purity flux used before.

2 Production

2.1 The Flux Method

The crystal growth technique more commonly used for oxide crystal growth for industrial and commercial ends is the Czochralski (CZ) Method [5]. This technique involves loading a seed crystal into a melt in a crucible that is slowly raised to grow the crystal [1]. While the CZ method allows the bulk production of high-quality crystals, this method requires higher temperatures in relation to the flux method. It is a highly complex technique, requiring a higher degree of expertise and specialised equipment, as opposed to the flux method, which allows the crystal formation with simple furnaces. Thus, it is of interest the development and improvement of the flux method as a Al_2O_3 crystal growth method.

The flux method is a technique used for crystal growth at temperatures below the melting point of the solute. This method uses slow-cooling, flux-evaporation or temperature-gradient techniques to achieve supersaturation states, which enable crystal growth at reduced temperatures [6].

In this project, the crystals grown are primarily of Al_2O_3, which has a melting point of 2072 ºC [7]. The chosen flux for this process was molybdenum trioxide (MoO_3) which was proven useful in ruby crystal growth, which are Al_2O_3 crystals doped with chromium (Cr_2O_3) [8]. MoO_3 evaporates at temperatures above 1050 ºC. Therefore, the use of this technique with a MoO_3 flux allows a significant decrease of the required temperatures to a range of 1050 - 1200 ºC. Due to the high volatility of MoO_3, the addition of evaporation inhibitors, such as Li_2O, decreases its evaporation rate, which allows a slower and more controlled growth [9, 10]. Earlier experiments have shown that a molar ratio of 85% MoO_3 to 15% Li_2O yielded crystals with fewer defects and more transparency. The choice of this specific ratio helps optimise both the stability of the growth process and the quality of the resulting crystals.

2.2 Methods

The mass of the MoO_3 (99%, Merck, Germany) and Li_2O (99.5%, Alfa Aesar, Thermo Fisher Scientific, EUA) reagents was measured to obtain a Li_2O-MoO_3 flux of

15 g, ensuring the molar ratio mentioned above. The mass of Alumina powder (99.99%, Alfa Aesar, Thermo Fisher Scientific, EUA) was measured to ensure a 7% mol ratio of the flux. The homogeneous mixture of the reagents was transferred to a 10 mL platinum crucible (Sigma Aldrich, Germany) and the crucible was inserted in a Horizontal Tubular Furnace with programmable digital temperature control (Termolab, Lda, Portugal). Initially, the temperature was increased at a controlled rate of 150 ºC/h until reaching the desired growth temperature, 1070 to 1180 ºC. This temperature was maintained for 48 hours before the furnace was cooled at a rate of 150 ºC/h, down to room temperature. Finally, the resulting crystals were isolated with hot water from the flux matrix. Note that a reducing atmosphere at a low partial pressure of oxygen is reported to stimulate the creation of oxygen vacancies [3], but for the current studies, no methods to control pressure or the atmosphere were used.

The exact temperature at which the crystals are grown is one of the most critical factors influencing their growth. The temperature has an effect on the rate at which the flux evaporates, and, consequently, the time and velocity of the growth, with higher temperatures leading to shorter and faster growth. In this paper, to study the effect of temperature on undoped Al_2O_3 crystal growth, three batches at different temperatures were produced.

2.3 Results

In Figure 1, it can be observed that the crystals grown at a temperature of 1140 ºC have higher quality. Even though the crystals grown at 1090 ºC are more similar to a bipyramid, the crystals present a darker colouration, that reduces the capacity to read luminescent signals. This darker colouration can be caused by irregularities during growth, leading to defects in the 3D matrix of the crystals. The crystals grown at 1180 ºC, are too small to be dosimeters, as a result of the faster growing conditions. In addition, these crystals presented the least bipyramidal geometry of the three batches.

The produced crystals were analysed through SEM Phenom ProX Desktop SEM (Thermofisher, USA) via energy dispersion spectroscopy (EDS), using 15 kV. In Figure 2, the expected ratio of O and Al in alumina is confirmed (60% O and 40% Al). The dopants weren't detected, because of the low sensitivity of SEM compared to their concentration. All crystals have well-defined faces and edges, although some aren't perfectly smooth. All the images show bright and dark spots, the former corresponds to crystals of molybdenum oxide that form on the surface and the latter to carbon impurities, which are superficial too.

(a) Images of 1090 ºC production and one example crystal

(b) Images of 1140 ºC production and one example crystal.

(c) Images of 1180 ºC production and one example crystal.

Figure 1: Production Results.

3 Absoption Spectrum

3.1 Theoretical Background

The α-Al_2O_3 has a rigid, slightly distorted hexagonal close-packed sublattice of O^{2-} ions with Al^{3+} ions occupying two out of every three octahedral interstices (fig. 3a). Each O^{2-} ion is surrounded by four tetrahedral nearest neighbour Al^{3+} ions.

Colours centers (F-centers or luminescent centers) are a type of punctual defect that can be caused by vacancies and impurities [1]. These defects disrupt the crystal's regular arrangement of atoms, which leads to localized energy states that absorb light at specific wavelengths, resulting in the observable colour centers. During the growth of Al_2O_3 crystals, oxygen vacancies are created, which are occupied by unpaired electrons and can be characterized by their number. The defects are denominated neutral F centers, when occupied by two electrons, identified by a strong absorption band at 205 nm and F^+ center when occupied by one electron, identified by two overlapping absorption bands at 230 and 255 nm. (Fig. 3b)

Additionally, for Al_2O_3:C,Mg crystals, the presence of Mg^{2+} ions originates F_2^{2+} centers, when two oxygen vacancies are charge-compensated by two Mg^{2+} ions, identified by a 435 nm absorption band. F_2^+ centers can also exist and are identified by bands at 335 and 620 nm [1]. It is possible other defects combinations (such as F^+(Mg), F^{2+}, etc...), but their effect is not significant compared to the previously mentioned F-centers [4].

In Figure 4, the most important phenomenon to the dosimeter capability of the crystals is illustrated. When irradiated F^+ and F_2^{2+} centers can undergo radiochromic

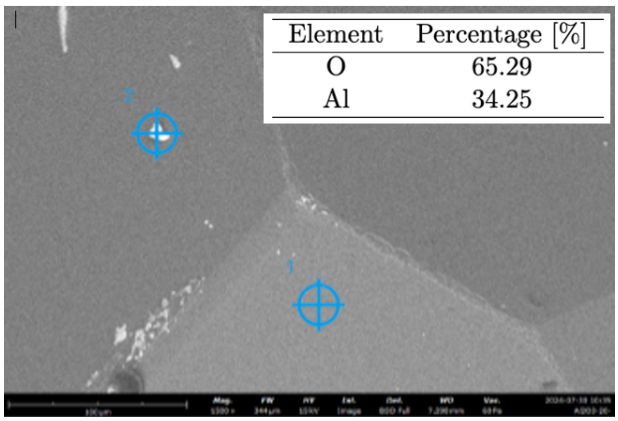

(a) 1090 ºC Crystal.

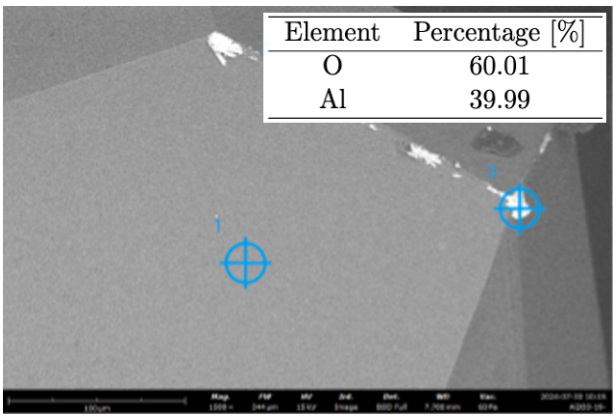

(b) 1140 ºC Crystal.

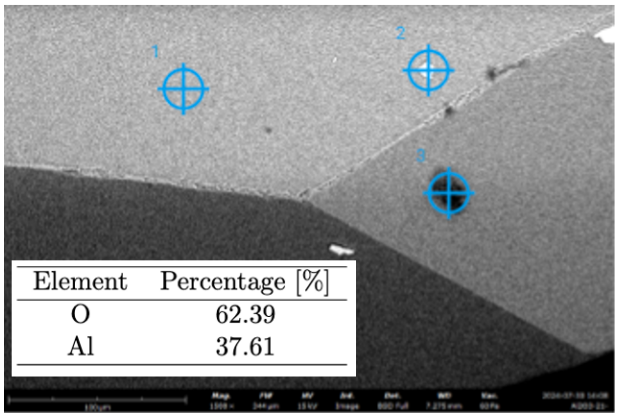

(c) 1180 ºC Crystal.

Figure 2: SEM results with an image of a crystal of each batch and respective elemental percentage in the matrix.

transformations gaining one electron, becoming F and F_2^+ centers.

3.2 Methods

The absorption spectra of the various crystals were acquired with a UV-Vis Spectrophotometer SHIMADZU UV-1280. The spectra ranged from 190 to 700 nm and were analysed with the UV Probe software. The sample holder was adapted with black tape to limit the absorption area, so it coincides with the crystal's dimensions, as shown in Figure 5.

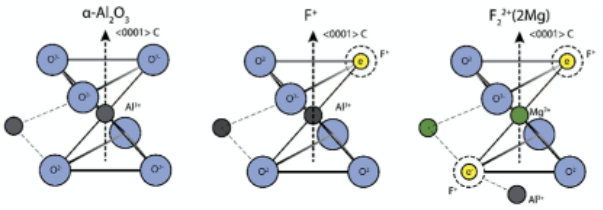

Figure 3: Lattice structure of α-Al_2O_3:C,Mg and its important defects, respectively: a) simplified ideal lattice cell, b) single oxygen vacancy with one electron – F^+ center and c) aggregate defect F_2^{2+}(2Mg)-center consistent of two oxygen vacancies (two F^+ centers) and charge compensated by two Mg^{2+}-ions [1].

Figure 5: Photo of the adapted support.

3.3 Results

The absorption spectra for the commercial Al_2O_3:C,Mg crystals non-irradiated and alpha or beta irradiated are presented in Figure 6. There are peaks at the expected wavelengths for F centers, F^+ centers and the F_2^{2+}, which are coincident with the reported by other studies [1, 3], as well as the shape of the spectrum.

The crystal irradiated with beta radiation also showed an absorbance peak at 335 nm, which corresponds to the F_2^+ centers. Their presence is caused by beta radiation, which should have triggered the radiochromic transformations of the F_2^{2+} centers into F_2^+. This transformation is further justified by a lower peak at 435 nm, which indicates a reduction in F_2^{2+} centers. Also, a change in the colour of the crystal could be directly observed, since the F_2^{2+} centers emit the radiation at 520 nm, the non-irradiated crystals have a yellow-green colour, but the irradiated crystal is paler. Moreover, it is observable a reduction in the F^+ centers, which could have become F-centers, due to a radiochromic transformation. Both transformations of the defects under radiation are in accordance with [4], where these effects are induced not by radiation but by laser bleaching, which is analogous.

In contrast, the absorption spectra for the Al_2O_3 crystals produced by us (example in Figure 7) presented a

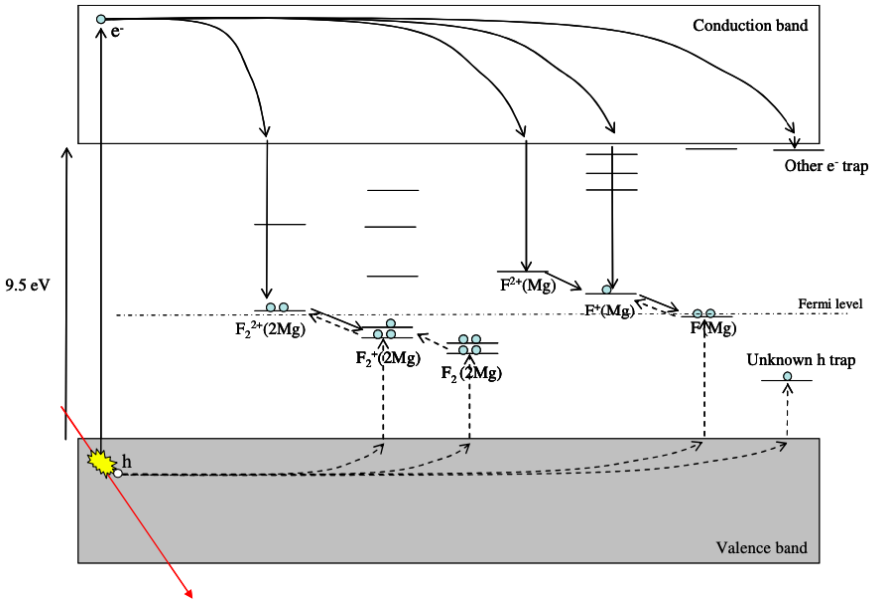

Figure 4: Flat band diagram of electron and hole trapping mechanisms in Al_2O_3:C,Mg after energy deposition by ionizing radiation. Solid lines represent electron related phenomenon and dashed lines represent hole related phenomenon [1].

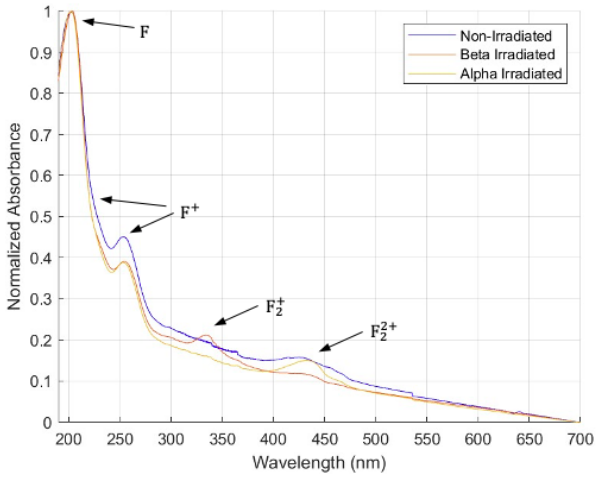

Figure 6: Normalized absorption spectra for the commercial Al_2O_3:C,Mg, irradiated and non-irradiated.

highly irregular shape, so it can only be said that they have approximately the expected behaviour, with an absorption region in the UV region, but it can't be made a quantitative analysis.

The main cause is expected to be the shape of the crystals, since ours were analyzed as shown in Figure 1, contrary to the commercial ones, which are laminated and polished. The irregular shape and higher thickness can cause diffraction that distorts the results. The absence of some expected peaks can also be due to the presence of the dark centers in the produced crystals and possible irregularities in the crystal matrix. Considering this, the first step in a future work should be the lamination of the produced crystals in order to eliminate any shape related effect.

4 OSL Analysis

4.1 Theoretical Background

Optical Stimulated Luminescence (OSL) is a stimulated phenomenon in condensed matter that can be used for passive integrating solid state dosimetry [3]. It's the transient luminescence that can be observed when crystalline insulators or semiconductors are excited by ionizing radiation (such as beta radiation) [11], which leads to a perturbation of the system from a state of thermodynamic equilibrium to a metastable state [3]. In this state, electrons and holes are trapped in the defects of the crystal lattice that are only released through light stimulation, during the OSL process. The release of the electrons and holes from these traps results in the recombination and excitation of the luminescence centers. What the OSL method analyses is the photons emitted during the decay of the luminescence centers to the ground state [11]. This process is schematized in Figure 8.

Continuous Wave Optical Stimulated Luminescence (CW-OSL) is a simple OSL technique that allows the use of simple instrumentation to acquire a good signal to noise ratio with a fast readout, making it the most common stimulation method for dosimetry and luminescence dating [12]. The light used to stimulate the detector is provided at constant intensity, allowing the discrimination between OSL and stimulation light based simply on wavelength separation. The separation of the wavelength is possible using wavelength filters for the OSL light measurement [11].

4.2 Methods

The OSL measurements were performed with a Risø TL/OSL DA reader (Risø National Laboratory, Denmark).

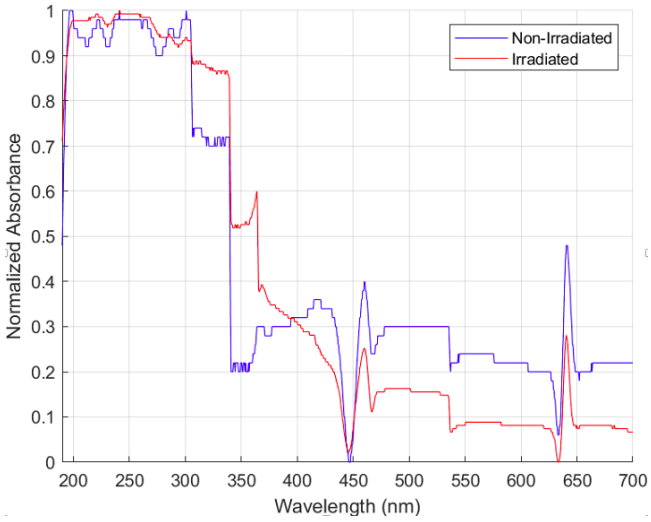

(a)

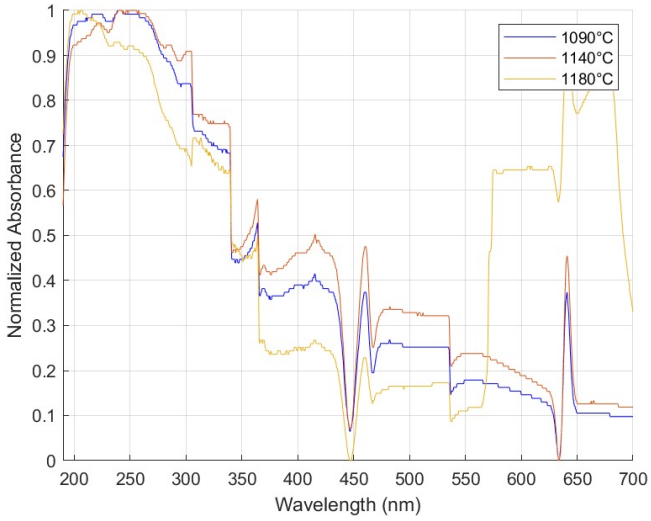

(b)

Figure 7: Absorption spectra for: a) Al_2O_3,C:Mg crystal produced with 99.5% flux, irradiated and non-irradiated. b) Al_2O_3 crystals produced to study growth temperature effect.

The luminescence efficiency was evaluated by exposing the Al_2O_3 crystals to a 90Sr/90Y beta radiation source with doses between 6.2 and 62 Gy (the source dose rate, 62 mGy/s, is calibrated for quartz grains). The OSL was performed in continuous wave mode at room temperature for 120 s, using blue LEDs (470 nm, FWHM = 20 nm, 80 mW/cm2 at the sample position) with a 60% of maximum LED power.

Initial thermal treatment was carried inside the Risø reader, from room temperature to 450 ºC at 5 ºC/s followed by cooling to room temperature. This ensured all traps were cleared by thermal annealing. Then OSL measurements were performed in crystals not irradiated (0 Gy) and then in the crystals irradiated for 100 s to 1000 s (6.2 Gy to 62 Gy). Between irradiations, after the crystal was

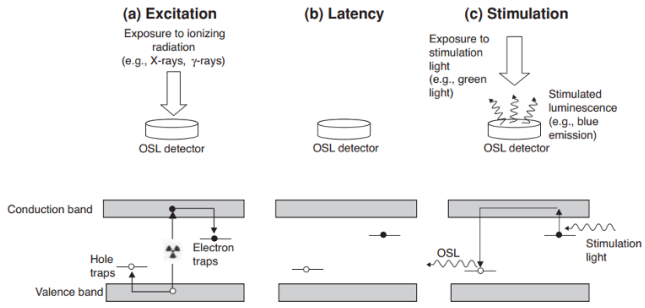

Figure 8: Different stages involved in the OSL process: (a) excitation of the OSL detector by ionizing radiation creating free electrons (•) and holes (○); (b) latency period characterized by a metastable concentration of electrons and holes captured at defects in the crystal and (c) stimulation of the detector with light, leading to recombination of electron–hole pairs and emission of light (OSL). The upper half represents the interaction of the detector with the ionizing radiation field and stimulation light; the bottom half represents the energy band diagram for the crystal with the available energy levels and corresponding electronic transitions occurring during each stage [11].

measured, the initial thermal treatment was performed to ensure the electrons from all remaining traps were cleared.

To block the stimulation light, preventing scattered stimulation light from reaching the PMT, the Risø reader was equipped with a UV-transmitting visible-absorbing filter that only allows the detection of light with a wavelength less than 400 nm (5.0 mm thickness Hoya U-340 detection filter).

The OSL data was recorded for 3 samples of each type of crystal, and then it was normalized to the mass of the sample. Also, it was considered the mean of the last 4.8 s (equivalent to 20 points of OSL data) to be the value of the background signal and subtract it from all the values. This treatment yields the results in Figure 10.

4.3 Results

4.3.1 OSL Curves

The OSL intensity decays with time non-linearly, so a single exponential (ae^{-bx}) and a double exponential ($a_1e^{-b_1x} + a_2e^{-b_2x}$) decay models were tested. Both models were evaluated using R^2 since it measures the total difference between the data points and the fit.

The best results were obtained with a double exponential, for example with the single exponential the worst R^2 of fit is 0.849 for Al_2O_3:C,Mn 0.77 mg, but the R^2 of the double exponential is 0.992, which is evident from Figure 9. The double exponential suggests the existence of fast and slow OSL traps.

In Figure 10, the first difference related to flux purity can be observed, the dispersion of the points around the trend line is lower for the two 99.5% purity flux crystals, making the uncertainty related to the fits and associated

results lower. The bigger dispersion in the 99% flux crystals could be caused by impurities that alter the distribution and energies of the OSL traps.

In Figure 11, the curves are normalised to the maximum intensity for each curve. There is a characteristic behaviour transversal between the 99.5% flux crystals, but in the 99% flux crystals, there isn't, which is not desirable. It's also observed, in the 99.5% flux crystals, that the OSL intensity decays faster for higher doses, indicating an OSL behaviour dependent on the dose.

The next two OSL characteristics analysed were the decay times and the integral of the fit for each dose. Since there are 3 samples for each type of crystal (x_i), it was used a weighted, by uncertainty (s_i), mean (equations 1 and 2) to obtain one unique value and uncertainty. This way it is ensured that the values with bigger uncertainty are not overrepresented.

$$\overline{x} = \frac{\sum^n \frac{x_i}{s_i^2}}{\sum^n s_i^{-2}} \tag{1}$$

$$s_{\overline{x}} = \sqrt{\frac{1}{\sum^n s_i^{-2}}} \tag{2}$$

4.3.2 Decay Times

The unit of the b constants have s^{-1} units, so it's inverse has s units and represents the decay time of the OSL traps. The two exponentials are associated with fast and slow traps, therefore there are fast and slow decay times. Although the double exponential fit is considered better, the decay time associated with the single exponential is also presented for reference.

All decay times were obtained with the inverse of the b constant and the uncertainties by error propagation of the fit uncertainty. Then it was applied equations 1 and 2 and the results in Figure 12 were obtained. The uncertainties have a maximum value of 0.1 s making them difficult to see directly from the graph.

The single exponential decay times should directly represent the faster decay to higher doses, decreasing with dose. As so, it decreases for the 99.5% flux crystals, but it increases with the dose for the 99% flux crystals. Therefore, the 99.5% flux has a better performance again.

However, the double decay times should be constant (independent of dose) since the faster total decay time is given by a larger contribution of the fast decay exponential. The ratio between the constant a_i associated with the fast decay exponential and the one associated with the slow decay exponential becomes larger with dose, but the b_i remains constant. As expected, the slow and fast decay times are constant for crystals of both fluxes, so they can be used to assess the quality of the crystals, as variation from a constant value could be due to impurities or unwanted defects.

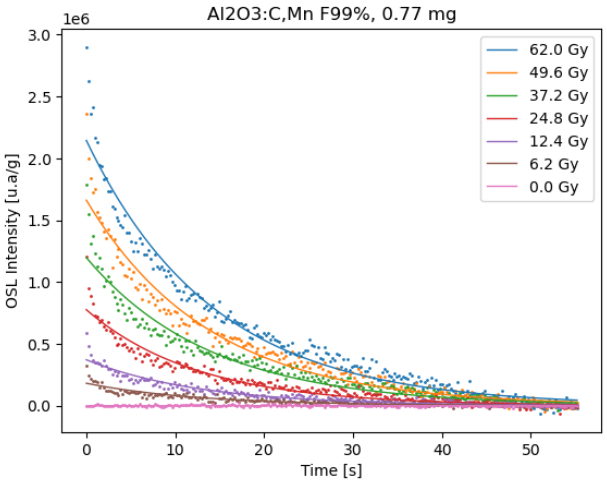

(a)

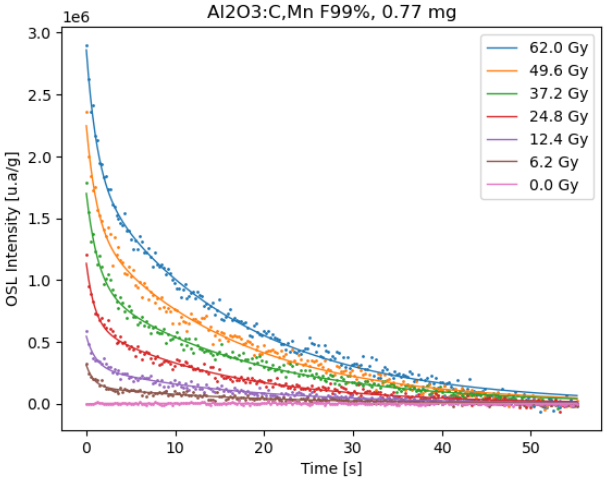

(b)

Figure 9: Comparison of mass-normalized OSL intensity of the 0.77 mg Al_2O_3:C,Mn crystal produced with 99% purity flux, fitted to a single exponential, a), and double exponential, b).

4.3.3 OSL Signal to Dose

The variation of the total OSL signal to dose is how these crystals can be used as dosimeters, so the value of the integral of the fit of the OSL signal was related to the respective dose, obtaining the results in Figure 13.

The crystals produced with the purest flux have a higher OSL signal: the Al_2O_3 crystal of lower purity has a signal that is 6% to 19% of the higher purity Al_2O_3 (the difference increases with dose) and, similarly, the Al_2O_3:C,Mg crystal of lower purity has a signal that is 3% to 12% of the higher purity crystal. These values indicate that even a 0.5% difference in flux purity has a significant impact on the total OSL signal because the impurities in the flux cause defects that compete with the OSL trap defects.

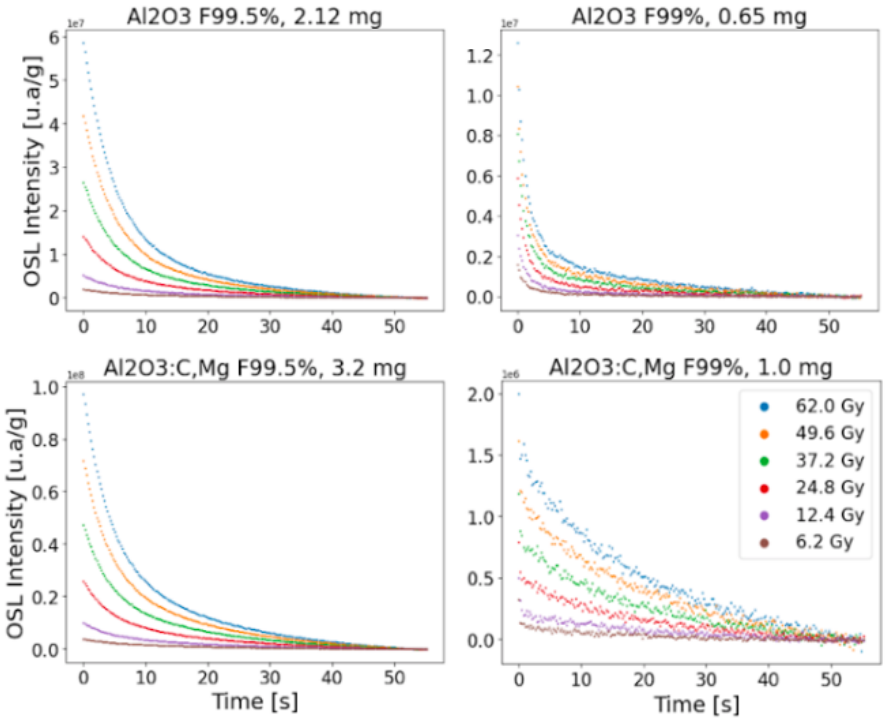

Figure 10: Mass-normalized OSL intensity for Al_2O_3 and Al_2O_3:C,Mg crystals, produced with 99% and 99.5% flux.

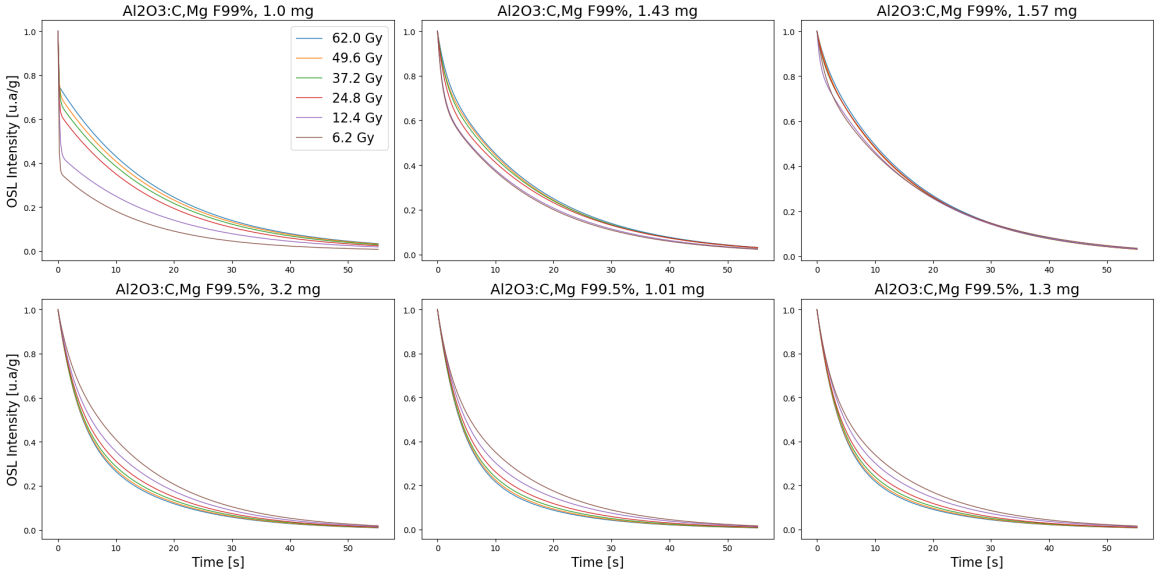

Figure 11: OSL Intensity double exponential fit normalized, for Al_2O_3:C,Mg produced with 99% and 99.5% flux as examples.

Another difference between fluxes is the regularity of the values, since in the 99% flux crystals the data of the comparable crystals is more irregular.

The second most important characteristic is the dopant combination. The only combinations with a clearly higher signal than the undoped Al_2O_3 are the C and Mg, with 99.5% flux, and C and Ti, with 99% flux. In the Al_2O_3:C,Mg case, the undoped crystal has an OSL signal between 65% and 77% of the doped crystal. In the Al_2O_3:C,Ti case, the undoped crystal signal is between 74% and 82% of the doped crystal.

Also in Figure 13, the points form a line with two slopes in a log-log graph, so there is one power behaviour (aD^b) for low doses (< 25 Gy) and other to high doses (for high doses OSL signal increases faster). Therefore, a fit of the 99.5% flux crystals OSL signal for each region was done with a linear regression of the function

$ln(y) = ln(a) + b\ ln(D)$. In Figure 14, the results are presented, where the described behaviour is clear.

In the table 1, are the parameters for each power fit, which were obtained from the linear regression parameters, the uncertainties are the propagation of the errors of the linear regression. There is a difference in the parameter b for low doses between the crystals, but this parameter is almost the same for high doses.

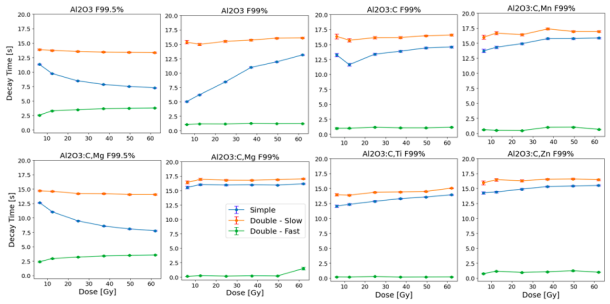

Figure 12: The decay times for each type of crystal produced.

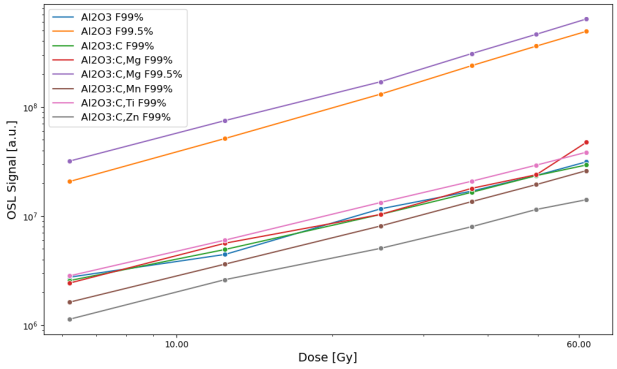

Figure 13: Dosimetric curves of each crystal, relating OSL signal to dose.

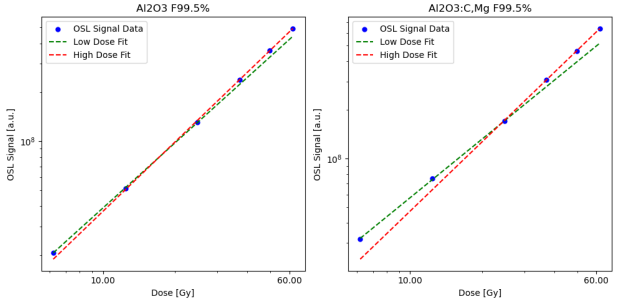

Figure 14: Power Fit of the OSL signal of the 99.5% flux crystals for low and high doses.

		Al_2O_3	Al_2O_3:C,Mg
Low Doses	a	$(1.82 \pm 0.06) \times 10^6$	$(3.5 \pm 0.2) \times 10^6$
	b	1.33 ± 0.02	1.21 ± 0.02
High Doses	a	$(1.42 \pm 0.06) \times 10^6$	$(1.76 \pm 0.07) \times 10^6$
	b	1.41 ± 0.01	1.42 ± 0.01

Table 1: Dose to OSL signal fit Parameters and uncertainties for the 99.5% flux crystals.

5 Conclusions

In this study, crystals were grown at different temperatures, with the best best results achieved for a growth temperature of 1140 ºC, because of the equilibrium between transparency and size of the crystals. The difference in the absorption spectra between the laminated commercial crystals and the produced crystals demonstrates their need to be laminated.

During the OSL analysis, we conclude that a double exponential is the best fit for the OSL intensity ($a_1 e^{-b_1 x} + a_2 e^{-b_2 x}$), the use of a higher purity flux leads to better OSLD characteristics (less dispersion of values, more regular behaviour between crystals and higher OSL signal), the dopant combination with higher OSL signal is C and Ti, and the dosimetric curve of the OSLD crystals is well-defined by two two power laws, one for low doses (<25 Gy) and other for high doses, but more data would contribute to better fits.

The more prominent future work objectives are to study Al_2O_3:C,Ti produced with 99.5% and 99.99% fluxes (although the other dopant combination should also be tested), analyse OSL signal in a wider dose range (below 6 Gy and above 60 Gy), and laminate our crystals to study their absorption spectra.

References

[1] M. Akselrod, J. Kouwenberg, Radiation Measurements **117**, 35 (2018)

[2] M.S. Akselrod, A.E. Akselrod, S.S. Orlov, S. Sanyal, T.H. Underwood, Journal of Fluorescence **13**, 503 (2003)

[3] M.S. Akselrod, A. Rosenfeld, T. Kron, F. d'Errico, M. Moscovitch, AIP Conference Proceedings (2011)

[4] G.J. Sykora, Ph.D. thesis, Oklahoma State University (2010)

[5] C. Brandle, Journal of Crystal Growth **264**, 593 (2004)

[6] S. Oishi, K. Teshima, H. Kondo, Journal of the American Chemical Society **126**, 4768 (2004)

[7] P. Patnaik, *Handbook of Inorganic Chemicals* (McGraw-Hill Professional, 2003), ISBN undefined

[8] S. Ayuzawa, S. Suzuki, M. Hidaka, S. Oishi, K. Teshima, Crystal Growth amp; Design **20**, 2019 (2020)

[9] N. Leonyuk, A. Lyutin, V. Maltsev, S. Barilo, G. Bychkov, L. Kurnevich, G. Emelchenko, V. Masalov, A. Zhokhov, Journal of Crystal Growth **280**, 551 (2005)

[10] K. Teshima, H. Kondo, S. Oishi, Bulletin of the Chemical Society of Japan **78**, 1259 (2005)

[11] S.W.M. E. G. Yukihara, *Optically Stimulated Luminescence: Fundamentals and Applications* (Wiley, 2011)

[12] N. Rawat, B. Dhabekar, M. Kulkarni, K. Muthe, D. Mishra, A. Soni, S. Gupta, D. Babu, Radiation Measurements **71**, 212 (2014)